



Title:

Enhanced Motion Planning for Differential Drive Mobile Robots Using C^1 -Continuous Double Clothoid Segments

Authors:

Mohd Fazril Izhar Mohd Idris, fazrilizhar@uitm.edu.my, Universiti Teknologi MARA, Perlis Branch
Ahmad Ramli, alaramli@usm.my, Universiti Sains Malaysia
Wan Zafira Ezza Wan Zakaria, ezzafira@usm.my, Universiti Sains Malaysia

Keywords:

Motion Planning, Differential Drive, Mobile Robot, Clothoid Segments

DOI: 10.14733/cadconfP.2024.318-323

Introduction:

Advancements in technology have driven a significant evolution in robotics, meeting the increasing need for robots adept at navigating intricate environments, crucial for their effectiveness and safety across various sectors like industrial automation, service robotics, and autonomous vehicles [7]. At the core of this capability lies motion planning, a fundamental process through which robots determine optimal trajectories to navigate from an initial state to a desired goal while avoiding collisions with obstacles [14].

The complexity of motion planning for differential drive robots arises from navigating a multi-dimensional state space to find trajectories that minimize cost functions while considering constraints like obstacle avoidance and the robot's kinematic limits [5], exacerbated by their non-holonomic nature, which restricts lateral movement [8], leading conventional algorithms like potential fields and rapidly exploring random trees (RRT) to struggle with generating smooth and efficient paths, especially in challenging environments with tight spaces or intricate geometries [1].

To overcome these challenges, we utilize Computer-Aided Geometric Design (CAGD), focusing specifically on Clothoid curves for motion planning, as they offer continuous and smooth curvature profiles, promising fluid robotic motion [3]. Our innovative approach integrates two clothoid curves, combining the unique features of both standard and mirrored clothoids. This article introduces a novel method employing double clothoid segments to enhance motion planning for differential drive mobile robots. We evaluate the effectiveness of this method by simulating robot trajectories in CoppeliaSim simulator platform, seamlessly integrated with the Matlab remote API and comparing them with prior studies [12] to assess trajectory smoothness, efficiency, and flexibility.

Mobile Robots:

The Pioneer 3-DX robot, made by Adept MobileRobots, is famous for its flexibility and reliability. It has two wheels that can move independently, allowing it to navigate precisely in any direction. This makes it great for tasks like navigation, surveillance, and research [13]. Its strong design is useful for many purposes in research, education, and industry. With its special steering system, it can easily move through tight spaces and tricky environments. It has sensors like lasers and cameras to see what is around it accurately. Plus, it is easy to add more sensors or gear to it.

However, it is noteworthy that this study implements a sensorless mode, foregoing the use of sensors typically found in the Pioneer 3-DX robot. Despite the absence of sensors, the robot's differential drive system still enables precise movements in various environments. In motion planning, these robots need smart algorithms to make smooth paths. New ideas like double clothoid segments can help improve how they plan their movements, making sure they move smoothly, especially in tight spots.

Methodology:

The Clothoid curve, alternatively referred to as the Cornu Spiral or Euler Spiral, is a mathematical construct characterized by a consistent rate of curvature [2]. Renowned for its unique geometric properties, this curve finds extensive applications in diverse fields such as road design, railway engineering, and robotics [4]. Its intrinsic ability to provide seamless transitions between curves of varying radii renders it indispensable in motion planning scenarios where gradual changes in curvature are imperative.

The standard parametric formulation of the clothoid curve was established by [9], which incorporates the Fresnel integral as the foundation for deriving the clothoid equation. Additionally, the generalization of the clothoid can be observed in the Aesthetic curve when $\alpha = -1$, which utilizes logarithmic functions as its basis in the formula [15]. Although both being capable of producing the same clothoid curve, these formulations stem from vastly different equations.

Clothoid formulation

The standard clothoid formulation [9], denoted as $C_s(t, \theta, i) = [X_s(t, \theta, i), Y_s(t, \theta, i)]$ is delineated by the following parametric equations:

$$X_s(t, \theta, i) = x_i + a_i [\cos(\theta) c(t) - \sin(\theta) s(t)], \quad (3.1)$$

$$Y_s(t, \theta, i) = y_i + a_i [\sin(\theta) c(t) + \cos(\theta) s(t)], \quad (3.2)$$

where $t \in R, 0 \leq \theta \leq \frac{\pi}{2}$ and i represent the i^{th} curve. Here, (x_i, y_i) denotes the initial point for the clothoid curve, while a_i signifies the scaling factor determined by the product of π, R_i and A_i with R_i representing the curve's radius and A_i is a positive parameter. The Fresnel integrals, $c(t)$ and $s(t)$ are integral components of clothoid formulation, defined as:

$$c(t) = \int_0^t \cos\left(\frac{\pi u^2}{2}\right) du. \quad (3.3)$$

$$s(t) = \int_0^t \sin\left(\frac{\pi u^2}{2}\right) du. \quad (3.4)$$

Conversely, the mirrored clothoid formulation, denoted as $C_m(t, \theta, i) = [X_m(t, \theta, i), Y_m(t, \theta, i)]$, represents a reflection of the standard clothoid across the x-axis, coupled with a rotation dependent on θ within the range of 0 to $\frac{\pi}{2}$, yielding:

$$X_m(t, \theta, i) = x_i + a_i [\cos(\theta) c(t) - \sin(\theta) s(t)], \quad (3.5)$$

$$Y_m(t, \theta, i) = y_i + a_i [-\sin(\theta) c(t) - \cos(\theta) s(t)], \quad (3.6)$$

where, (x_i, y_i) denotes the initial point for the mirrored clothoid curve, while a_i signifies the scaling factor determined by the product of π, R_i and A_i . A mirrored clothoid can be visualized as the reflection of the standard clothoid across the line $y = x$, achieved by setting the rotation angle to $\frac{\pi}{2} - \theta$, where θ represents the angle of the standard clothoid from the x-axis. This alternative representation simplifies the determination of mirrored clothoids. The incorporation of mirrored clothoids enables the development

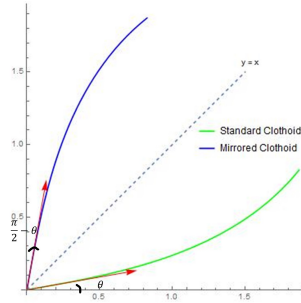


Fig. 1: Standard and mirrored clothoids.

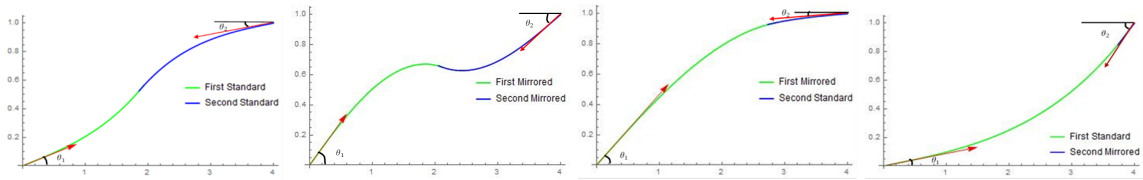


Fig. 2: Illustration of four variations of double clothoid segments, showcasing specific examples of tangent angles, θ at the starting and ending points. The figures are arranged from left to right. These variation include: (a) Both Standard Clothoids ($\theta_1 = 10^\circ, \theta_2 = 5^\circ$), (b) Both Mirrored Clothoids ($\theta_1 = 60^\circ, \theta_2 = 20^\circ$), (c) Mirrored-Standard Clothoids ($\theta_1 = 65^\circ, \theta_2 = 2^\circ$) and (d) Standard-Mirrored Clothoids ($\theta_1 = 5^\circ, \theta_2 = 30^\circ$).

of double clothoid segments, wherein they can be combined with other clothoids. Fig. 1 provides a visual representation of standard and mirrored clothoids.

Double Clothoid Segments

Our novel clothoids approach encompasses four distinct categories, each offering unique characteristics and applications: both standard clothoids, both mirrored clothoids, mirrored-standard clothoids and standard-mirrored clothoids.

These categories are visually represented in Fig. 2, showcasing the distinct characteristics and applications of each configuration. While this study closely aligns with the approach of combining two clothoids as seen in [6] and [10], there are differences in the method used to generate mirrored segments. In [10], clothoid splines were created using the control polyline technique, pairing clothoids as blending curves. Our study diverged by using a straight line $x=y$ for reflection, offering flexibility in determining tangent direction at both start and end points of movement, unlike prior methods.

The procedure for generating these double clothoids is based on equation from (3.1) to (3.6). The second clothoid segment, D_2 is derived from the first segment, D_1 through a sequence of transformations, including rotation, translation and reflection. Both D_1 and D_2 can be represented as either standard clothoids, C_s or mirrored clothoids, C_m . Specifically, D_1 that connected to (x_1, y_1) can be expressed as follows: $D_1(t, \theta, 1) = [X_s(t, \theta, 1), Y_s(t, \theta, 1)]$ or $[X_m(t, \theta, 1), Y_m(t, \theta, 1)]$ while D_2 that connected to (x_2, y_2) can be written as follows: $D_2(t, \theta, 2) = [X_s(t, \theta + \pi, 2), Y_s(t, \theta + \pi, 2)]$ or $[X_m(t, \theta + \pi, 2), Y_m(t, \theta + \pi, 2)]$.

To optimize the combinations of these clothoids, we employ a rigorous approach based on two funda-

mental conditions:

$$D_1(A_1, \theta_1, 1) = D_2(A_2, \theta_2, 2). \quad (3.7)$$

$$D_1'(A_1, \theta_1, 1) = -D_2'(A_2, \theta_2, 2). \quad (3.8)$$

Equation (3.7) marks the first condition emphasizes the importance of ensuring C^0 continuity, ensuring a seamless connection between clothoid segments. Subsequently, Equation (3.8), the second condition ensures C^1 continuity, which dictates a smooth transition in tangent directions between the segments. These conditions are pivotal in guiding the determination of four critical parameters: the radii of curvature for the first and second clothoids (R_1, R_2), and the parameters A_1 and A_2 , all of which are constrained to be greater than zero to maintain the validity of the clothoid curves.

In our study purpose, we preserve C^1 continuity for motion planning as seen in Equation (3.8), ensuring smooth direction changes at junction points, ideal for basic point-to-point navigation. While G^2 continuity promises even smoother transitions in curvature rates, making trajectories exceptionally seamless, we opted for C^1 for its simplicity and effectiveness. Nonetheless, we envision implementing a G^2 continuous path in our future studies.

To effectively solve for these parameters, various numerical methods can be employed. One efficient approach is through the utilization of built-in functions in software packages such as Mathematica. These tools offer computational capabilities that expedite the parameter-solving process, facilitating rapid and accurate determination of the clothoid parameters.

Result and Discussion:

We illustrate the process of selecting viable and appropriate categories based on the chosen tangent angles for the beginning, represented by θ_1 and end, θ_2 of the trajectory. Subsequently, we present the simulation results of robot movements based on all four categories of double clothoid segments. Finally, we compare these results with previous study based on categories suitable for the trajectories created in this study.

Selection of Double Clothoid Segment Categories

This study is able for users to flexibly determine the tangent direction for robot trajectory movements at the starting and ending points. However, at present, it still requires a manual process to determine the appropriate category to be selected based on these chosen angles. In this study, we experimented with the starting point (0,0) and the ending point (4,1) across various tangent angles. The suitability of double clothoid segment categories was based on the obtained solutions if both clothoids were connected and were not selected due to the lack of solutions obtained.

For discussion purpose, we choose a case where $\theta_1 = 25^0$ and $\theta_2 = 15^0$. It is worth noting that only the both mirrored clothoid category provided solutions in this instance. Conversely, the other categories did not yield any values for the parameters, suggesting a lack of continuity between the two curvature segments for those categories, as shown in Fig. 3.

Simulated Result of Differential Drive Robot

We conducted several simulations on the movement of the Pioneer 3DX robot using the CoppeliaSim simulator platform for each category of double clothoid segments. Here, we assess whether the robot can follow the path generated from these double clothoid segments. Minor errors or discrepancies may arise due to various factors, as stated in [11] and [12]. However, overall, the robot's movement remains within the intended trajectory and final target point. Fig. 4 depicts one simulation for the θ 's defined above on the both mirrored category where the robot requires to make a turn the right before turning to the left. Even if the robot has to turn, then the simulated path is still close.

Comparison with Previous Study

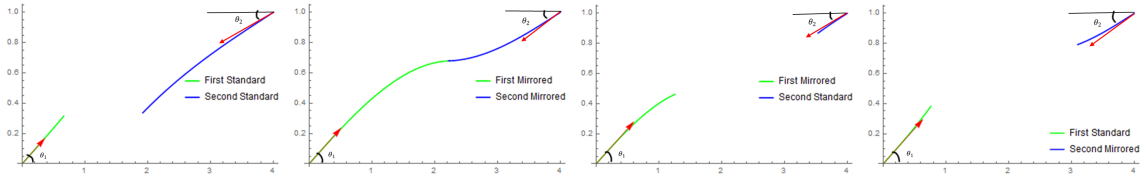


Fig. 3: The figures are arranged from left to right. These variations include: (a)Both Standard Clothoids (unsolvable), (b)Both Mirrored Clothoids (solvable), (c)Mirrored-Standard Clothoids (unsolvable), and (d)Standard-Mirrored Clothoids (unsolvable).

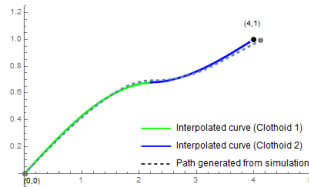


Fig. 4: Visualization of robot simulation on both mirrored clothoids based on Fig. 3(b).

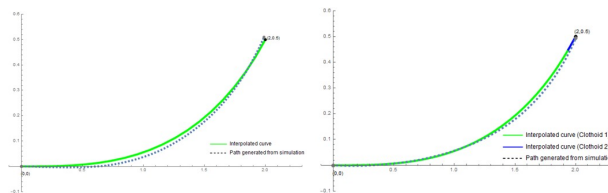


Fig. 5: Left: Simulation based on [12]; Right: Simulation using double clothoid segments by standard-mirrored clothoids' category.

The preceding study conducted by [12] addressed scenarios where point interpolation depended on a single standard clothoid curve. In such cases, determining the tangent angle at the initial point posed no significant challenge. However, computing the tangent at the target point required subsequent computation. This intricate process entailed integrating the parameter A into the differentiation of $C_s(t, \theta, 1)$, expressed as $C'_s(A, \theta_1, 1) = (p, q)$, followed by $\tan^{-1}(\frac{q}{p})$ to ascertain the tangent angle. Notably, in this instance θ_1 is set to 0^0 , while θ_2 is assigned 42^0 . The interpolated path alongside the simulated path is illustrated in Fig. 5, effectively showcasing the outcomes of the analysis.

Conclusion:

We introduce our inventive strategy in clothoids through the integration of double clothoid segments, simplifying calculation process despite the inherent complexity of clothoid formulations. This approach enhances trajectory planning by enabling straightforward determination of the tangent direction for both the initial and final points of robot movement. Such simplicity proves invaluable in navigating the intricacies of the robotic landscape, empowering robots to tackle even the most formidable challenges with ease.

Mohd Fazril Izhar Mohd Idris, <https://orcid.org/0009-0008-5231-3785>

Ahmad Ramli, <https://orcid.org/0000-0003-0853-3920>

Wan Zafira Ezza Wan Zakaria, <https://orcid.org/0000-0002-6421-840X>

References:

- [1] Chi, P.; Wang, Z.; Liao, H.; Li, T.; Tian, J.; Wu, X.; Zhang, Q.: AM-RRT*: An Automatic Robot Motion Planning Algorithm Based on RRT, International Conference on Neural Information Processing, 2023, 91-103. https://doi.org/10.1007/978-981-99-8079-6_8
- [2] Connor, D.; Krivodonova, L.: Interpolation of two-dimensional curves with Euler spirals, Journal of Computational and Applied Mathematics, 261, 2014, 320-332. <https://doi.org/10.1016/j.cam.2013.11.009>
- [3] Ishikawa, H.; Noguchi, K.; Maki, R.; Naitoh, H.: Path Generation with Clothoid Curve Using Image Processing for Two-Wheel-Drive Autonomous Mobile Robots, IFAC Proceedings Volumes, 42(16), 2009, 523-528. <https://doi.org/10.3182/20090909-4-JP-2010.00089>
- [4] Lin, P.; Javanmardi, E.; Tsukada, M.: Clothoid Curve-based Emergency-Stopping Path Planning with Adaptive Potential Field for Autonomous Vehicles, 2023. <http://arxiv.org/abs/2308.10049>
- [5] Loganathan, A.; Ahmad, N. S.: A systematic review on recent advances in autonomous mobile robot navigation. Engineering Science and Technology, an International Journal, 40, 2023, 101343. <https://doi.org/10.1016/j.jestch.2023.101343>
- [6] Meek, D.S.; Walton, D.J.: Offset curves of clothoidal splines. Computer-Aided Design, 22(4), 1990, 199-201. [https://doi.org/10.1016/0010-4485\(90\)90048-H](https://doi.org/10.1016/0010-4485(90)90048-H)
- [7] Othman, N. A.; Reif, U.; Ramli, A.; Misro, M. Y.: Manoeuvring speed estimation of a lane-change system using geometric hermite interpolation, Ain Shams Engineering Journal, 12(4), 2021, 4015-4021. <https://doi.org/10.1016/j.asej.2021.02.027>
- [8] Sani, M.; Hably, A.; Robu, B.; Dumon J.; Meslem, N.: Real-time Dynamic Obstacle Avoidance for A Non-holonomic Mobile Robot, 2023 IEEE 32nd International Symposium on Industrial Electronics (ISIE), Helsinki, Finland, 2023, 1-6. <https://doi.org/10.1109/ISIE51358.2023.10227920>
- [9] Vazquez-Mendez, M. E.; Casal, G.: The Clothoid Computation: A Simple and Efficient Numerical Algorithm, Journal of Surveying Engineering, 142(3), 2016. [https://doi.org/10.1061/\(ASCE\)SU.1943-5428.0000177](https://doi.org/10.1061/(ASCE)SU.1943-5428.0000177)
- [10] Walton, D. J.; Meek, D. S.: A controlled clothoid spline. Computers and Graphics, 29(3), 2005, 353-363. <https://doi.org/10.1016/j.cag.2005.03.008>
- [11] Wan Zakaria, W. Z. E.; Ramli, A.; Misro, M. Y.; Ab Wahab, M. N.: Motion Planning of Differential Drive Mobile Robot Using Circular Arc, Engineering Letters. 32(1), 2024, 160-167.
- [12] Wan Zakaria, W. Z. E.; Ramli, A.; Reif, U.: Motion Planning of Differential Drive Mobile Robot Using Clothoid. (Submitted for publication).
- [13] Webots documentation, Adepts Pioneer 3-DX, Accessed: Feb. 14, 2024. <https://www.cyberbotics.com/doc/guide/pioneer-3dx?version=R2021a>
- [14] Yang, Y.; Pan, J.; Wan, W.: Survey of optimal motion planning, IET Cyber-systems and Robotics, John Wiley and Sons Inc, 1(1), 2019, 13-19. <https://doi.org/10.1049/iet-csr.2018.0003>
- [15] Yoshida, N.; Saito, T.: Interactive aesthetic curve segments, The Visual Computer, 22, 2006, 896-905. <https://doi.org/10.1007/s00371-006-0076-5>